Queued quantum collision models

Guilherme Fiusa[1] and Gabriel T. Landi[1]

[1]*Department of Physics and Astronomy, University of Rochester, Rochester, New York 14627, USA**

(Dated: March 29, 2024)

Collision models describe the sequential interactions of a system with independent ancillas. Motivated by recent advances in neutral atom arrays, in this Letter we investigate a model where the ancillas are governed by a classical controller that allows them to queue up while they wait for their turn to interact with the system. The ancillas can undergo individual open dynamics while they wait, which may cause them to decohere. The system, which plays the role of the server in the queue, can also undergo its own open dynamics whenever it is idle. We first show that this framework generalizes existing approaches for quantum collision models, recovering the deterministic and stochastic formulations in the appropriate limits. Next, we show how the classical queueing dynamics introduces non-trivial effects in the quantum collisions, that can lead to different phases in the system-ancilla response. We illustrate the idea with a model of coherence transfer under noisy waiting dynamics.

Introduction.–Open quantum systems traditionally describe the interaction with a many-body reservoir, whose properties are not very controllable. However, advances in quantum-coherent platforms motivate the design of synthetic open dynamics, in which the environment is highly structured. The canonical example is cavity QED [1, 2], in which the environment is a stream of atoms that are sent toward a cavity in an orderly fashion. Other important examples include cascaded quantum systems [3–5], squeezed baths [6, 7] and dispersive resonator couplings [8–11]. Recent experiments with neutral atom arrays [12–16] have taken this a step further and demonstrated the efficient use of classical controllers, which can physically move qubits at will, in order to put them in contact so that they can interact. These results motivate furthering our understanding of new types of engineered open dynamics.

An approach that has enjoyed significant success in this respect are the so-called quantum collision models (QCMs) [17–31], in which a central system interacts sequentially with arriving ancillas, one at a time (Fig. 1(a,b)). QCMs replace the complex system+bath evolution with a simpler dynamics involving only two bodies, at any given time. Moreover, they allow for fine control over energetics and memory effects, making them ideal for benchmarking e.g. thermodynamics [18, 32–35], and non-Markovianity [36–40]. For this reason, in the past they have been used in various tasks, such as metrology/thermometry [22, 41–45], and in the modeling of continuous measurements [46–48].

QCMs come in two standard flavors [23]. The first, called stochastic QCMs (Fig. 1(a)), is motivated by Boltzmann's molecular chaos hypothesis. It consists of a system that evolves unitarily by itself but is also subject to random collisions by arriving ancillas. The interarrival times of the ancillas are random, the duration of the collision process is short and, afterwards, the ancillas leave the process and never interact with the system again. The second are called the deterministic QCMs, in which there is an infinite "conveyor belt" of ancillas, usually prepared in identical states. Each ancilla interacts with the system for a fixed duration, after which they leave and never participate again in the dynamics (Fig. 1(b)). The reduced dynamics of the system is therefore stroboscopic. This kind of model fits naturally into a cavity QED scheme [49–51]. It also appears as the discrete-time picture of a system interacting with a chiral waveguide [52].

Both types of collision models can be imagined as particular cases of a more general scenario, in which a classical controller physically moves the ancillas according to some protocol. This will be the basic paradigm we adopt in this Letter. The system-ancilla interaction is quantum. But the way in which the ancillas are brought close to the system is classical, governed by an external controller. In neutral atom arrays, this paradigm is the backbone of any quantum computation [12–15]. Our interest here will be in the different types of dynamical behaviors that it may lead to.

More specifically, we consider in this Letter a queued version of the QCM. The rules are the following (Fig. 1(c)). The system still interacts with the ancillas one at a time. The duration of that interaction may vary from one ancilla to the other, either randomly or deterministically. Ancillas arrive according to some classical protocol, which can also be deterministic or stochastic. The main ingredient in the model is the assumption that if the system is occupied when an ancilla arrives, that ancilla will queue up, and wait for its turn. As we will show, this simple dynamical rule naturally interpolates between the stochastic and deterministic QCMs (Figs. 1(a,b)). Next, what will make this dynamical model particularly rich is the fact that, while the ancillas wait in the queue, they can undergo their own dynamics. For example, ancillas that are initially coherent might dephase depending on how long they wait. Similarly, whenever the system is idle – i.e. there are no ancillas available to interact with – it might also undergo its own dynamics.

We will show that this competition between the system-ancilla interactions and their individual waiting/idle dynamics leads to a rich set of dynamical behaviors, including different phases in the system-ancilla response. This will be illustrated with a toy model in which the ancillas are meant to transfer their initial coherence to the system, and both may undergo decohering effects while they are waiting/idle.

Queueing theory.–The classical controller governing the queue of ancillas follows the basic rules of single server queueing, with a first come, first serve discipline [53–55]. The system plays the role of a server, while the ancillas play the role of customers arriving in the queue, labeled as $n = 1, 2, 3, \cdots$, based on the order in which they arrive. We let T_n denote the interarrival time between ancilla n and $n+1$, with $T_1 = 0$. And we let S_n denote the time the system spends serving/interacting with ancilla n (see Fig. 1(d)). The set of times $\{T_n, S_n\}$ completely specifies the classical queueing dynamics, as all other stochastic quantities that may be of interest are entirely determined by this set. No assumptions need to be made about the structure of the $\{T_n, S_n\}$: they can be deterministic or stochastic, and they can be statistically independent or correlated [56].

The time the n-th ancilla waits in the queue is denoted as W_n^q. We define I_n as the idle time of the system after the $(n-1)$-th ancilla leaves and before the n-th ancilla arrives. The symbols are explained in Fig. 1(d). Importantly, W_n^q and I_n can be zero. For example, an ancilla might arrive to find the system idle, so it does not have to wait ($W_n^q = 0$). If the ancilla n has already arrived when the system is done with ancilla $n-1$, the system will have no idle time ($I_n = 0$).

Both W_n^q and I_n are fully specified from the set $\{T_n, S_n\}$ using Lindley's recursion relations [57]:

$$W_{n+1}^q = \max\{0, W_n^q + S_n - T_n\}, \tag{1}$$

$$I_{n+1} = \max\{0, -(W_n^q + S_n - T_n)\}, \tag{2}$$

where $W_1^q \equiv 0$ (the first customer always finds the queue empty) and $I_1 \equiv 0$. These relations can be intuitively understood from the diagram in Fig. 1(d). It is clear from this that $W_n^q I_n = 0$, meaning either there is no waiting for the ancilla or no idleness for the system. See Supplemental Material [58] for a comprehensive discussion about the statistics of waiting times W_n^q and idle times I_n.

The absolute time at which the n-th ancilla arrives in the queue is $t_n = \sum_{j=1}^{n-1} T_j$, and the absolute time when it leaves is

$$s_n := \sum_{j=1}^{n} (I_j + S_j), \tag{3}$$

which is nothing but the sum of all previous service and idle times of the system, up to n. The number of ancillas in the queue, at any given time, is depicted pictorially in Fig. 1(e). It will generally fluctuate with time and, during certain periods, drop down to zero [59]. The queue evolution therefore breaks down into busy periods and idle periods.

Queued QCMs.–We assume all ancillas arrive in the queue prepared in the same state ρ_A. While they wait, they may undergo a generic quantum channel $\mathcal{E}_A(W_n^q)[\rho_A]$ that depends on their waiting time W_n^q. Similarly, if the system is idle, it may undergo its own quantum channel $\mathcal{E}_S[I_n](\rho_S)$, which depends on the idle time I_n. If $W_n^q = 0$ or $I_n = 0$, their corresponding channels are assumed to reduce to the identity. Finally, the system-ancilla interaction is modeled by a channel $\mathcal{U}_{SA}(S_n)(\rho_S \otimes \rho_A)$ that depends on the service time S_n (see Fig. 1(c)). A pictorial representation of the response of the system to the fluctuating number of ancillas in the queue is shown in Fig. 1(f). During idle periods, the system evolves according to $\mathcal{E}_S$. During busy periods, it evolves according to a series of $\mathcal{U}_{SA}$ maps (we assume that as soon as an ancilla leaves, the next starts interacting with the system immediately if there are ancillas in the queue).

From a modeling perspective, it is more tractable to describe the system in discrete steps, only at the times each ancilla leaves the process. Let $\rho_S^n = \rho_S(s_n)$ denote the state of the system after the n-th ancilla leaves (which occurs at absolute time s_n, Eq. (3)). With the above definitions, one may readily write down a dynamical map connecting ρ_S^n with ρ_S^{n-1}:

$$\rho_S^n = \mathrm{Tr}_A\left\{\mathcal{U}_{SA}(S_n)\left[\mathcal{E}_S(I_n)[\rho_S^{n-1}] \otimes \mathcal{E}_A(W_n^q)[\rho_A]\right]\right\}, \tag{4}$$

where $\mathrm{Tr}_A\{\cdot\}$ denotes the partial trace over the ancilla. This map completely specifies the single-shot dynamics of the system, within a single realization of the queue. In general, there is no closed equation for the ensemble-averaged ("unconditional") evolution, which therefore has to be computed by numerically averaging Eq. (4) over different realizations of the queue. As our first result, we show how the map (4) recovers the stochastic and deterministic QCMs as particular cases.

Heavy traffic and deterministic QCMs.– The deterministic QCM in Fig. 1(b) is recovered in the "heavy traffic" limit, where $S_n \gg T_n$. This means that ancillas arrive much more quickly than the system can serve them. As a consequence, the queue quickly builds up, and the system will never be idle ($I_n = 0$), so $\mathcal{E}_S$ is the identity. To recover the standard formulation of deterministic QCMs, we must further assume that all service times are equal and deterministic, $S_n = \tau_{SA}$. The system-ancilla map is often assumed to be unitary, of the form $\mathcal{U}_{SA}(\tau_{SA})[\bullet] = e^{-iH_{SA}\tau_{SA}} \bullet e^{iH_{SA}\tau_{SA}}$, where H_{SA} is the system-ancilla Hamiltonian. However, this need not be the case in general. As a last ingredient, if we want all ancillas to start their interactions with the system in the same state, we must take $\mathcal{E}_A$ as the identity. Under these assumptions Eq. (4) reduces to

$$\rho_S^n = \mathrm{Tr}_A\left[\mathcal{U}_{SA}(\tau_{SA})(\rho_S^{n-1} \otimes \rho_A)\right], \tag{5}$$

while Eq. (3) reduces to $s_n = n\tau_{SA}$. Hence this recovers exactly the "conveyor belt" stroboscopic system dynamics [58].

Rare arrivals and stochastic QCMs.–The stochastic model in Fig. 1(a) is obtained in the regime of "rare arrivals", where $T_n \gg S_n$. In this limit, the recursion relation (2) implies that $W_{n+1}^q \simeq 0$ and $I_{n+1} \simeq T_n$. The ancillas therefore have no waiting time. The system is evolving, most of the time, under the idle map $\mathcal{E}_S(T_{n-1})$, which now depends only on the interarrival times T_{n-1}. For the model to remain interesting, one must assume that $\mathcal{U}_{SA}(S_n) = \mathcal{U}_{SA}$ is still non-trivial, even if S_n is very small. For example, a typical assumption is that $\mathcal{U}_{SA}$ is generated by a delta-like Hamiltonian, and is therefore independent of the actual value of S_n [28, 60].

A more common representation of stochastic QCMs is obtained if one switches to a time ensemble, where the system state is described at a fixed time, but the number of collisions can vary. This way, one obtains the evolution of

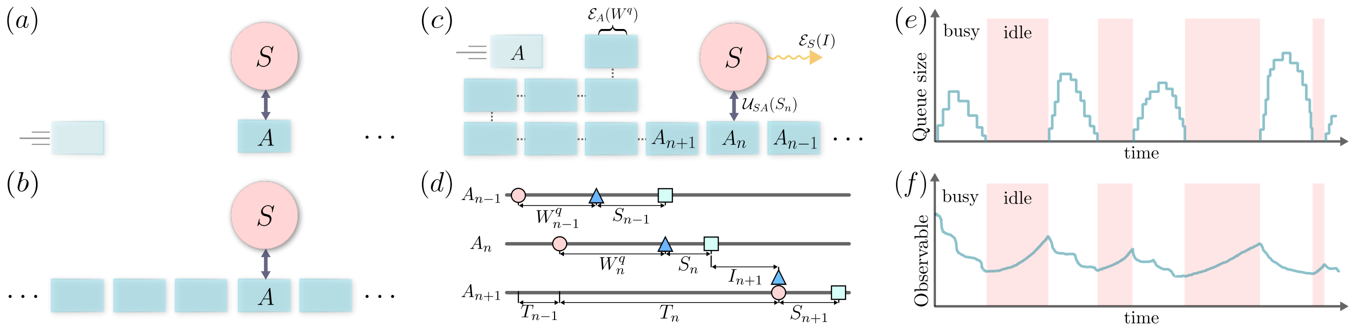

FIG. 1. Quantum collision models (QCMs), where a system interacts sequentially with arriving ancillas. (a) Stochastic QCM, where ancillas arrive according to a random interarrival distribution. (b) Deterministic QCM, where a "conveyor belt" of ancillas interacts stroboscopically with the system, at regular intervals. (c) The queued QCM introduced in this letter. The system interacts with the ancilla via the quantum channel $\mathcal{U}_{SA}$. If an ancilla arrives and another one is already interacting with the system, it will queue up and wait for its turn. While they wait, ancillas can undergo a quantum channel $\mathcal{E}_A$ that depends on the time spent in the queue W_n^q. If no ancillas are waiting, the system becomes idle and goes through a quantum channel $\mathcal{E}_S$ that depends on the idle period duration I_n. (d) Circuit diagram describing the main quantities in a classical queueing dynamics. Circles represent the ancilla's arrivals, triangles describe the beginning of the system-ancilla interaction and squares represent the ancilla's departures. The waiting and idle times W_n^q and I_n are determined from the interarrival and service times T_n and S_n through the Lindley recursion relations (1) and (2). (e) Schematic depiction of the random queue size over time, displaying busy and idle periods of the server (system). (f) Schematic depiction of a system observable over time, displaying how it responds differently to idle dynamics and system−ancilla interactions.

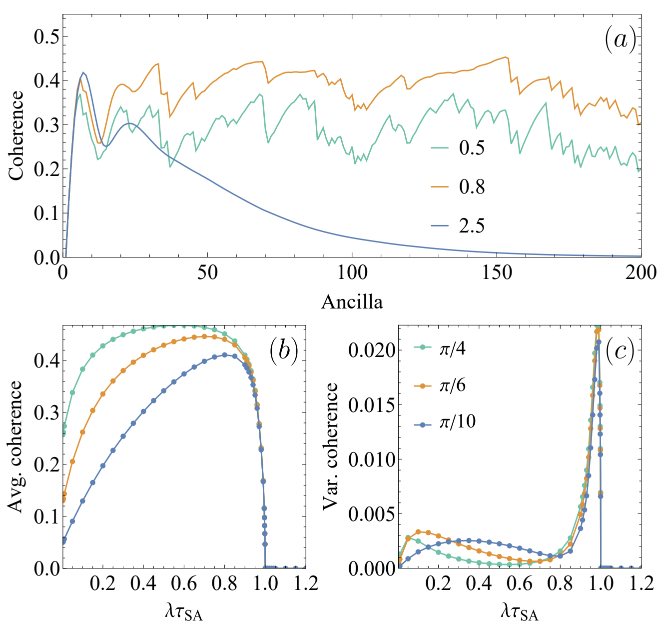

FIG. 2. System ℓ_1 norm of coherence C in the qubit toy model. (a) C_n as a function of ancilla number (evaluated at the times each ancilla leaves the process), for different values of $\lambda\tau_{SA}$, with $\gamma\tau_{SA} = 0.05$ and $g\tau_{SA} = \pi/12$. (b) Single-shot time average and (c) variance of the coherence in the long-time limit as a function of $\lambda\tau_{SA}$, for different values of $g\tau_{SA}$, with $\gamma\tau_{SA} = 0.05$.

an unconditional state. We show in [58] that the queued framework (Eq. (4)) recovers exactly this case. In particular, if T_n follows an exponential distribution, the unconditional state evolves under a time-local quantum master equation [28, 60]. Otherwise, the unconditional dynamics is generally non-Markovian [30, 61].

Competing dynamics.−Having shown how the map (4) contains the standard QCM formulations as particular cases, we move on to discuss how the competing effects between system-ancilla interactions ($\mathcal{U}_{SA}$) and individual waiting/idle dynamics ($\mathcal{E}_{A/S}$) give rise to a rich dynamics. To that end, we consider a model where the system and ancillas are qubits, which exchange excitations via a partial SWAP unitary $\mathcal{U}_{SA}(S_n)[\rho_S \otimes \rho_A] = U_{S_n}(\rho_S \otimes \rho_A)U_{S_n}^\dagger$, where $U_{S_n} = i\cos(gS_n) + \sin(gS_n)U_{\tt swap}$. Here g controls the strength of the interaction and $U_{\tt swap}$ is the full SWAP. The ancillas are prepared in $\rho_A = |+\rangle\langle+|$, where $|+\rangle = (|0\rangle + |1\rangle)/\sqrt{2}$ and $|0/1\rangle$ are the eigenstates of the Pauli matrix σ_z. The partial SWAP dynamics therefore transfers some of the coherence from the ancillas to the system. In the absence of $\mathcal{E}_{A/S}$ this reduces (irrespective of the queueing properties) to the homogenization problem of Ref. [18] where, in the long run, the system converges (homogenizes) to the ancilla's state.

We assume that while the ancillas wait in the queue or while the system is idle, they can both decohere. We model this as a dephasing channel $\mathcal{E}(t)[\rho] = \frac{1}{2}[(1 + e^{-\gamma t})\rho + (1 - e^{-\gamma t})\sigma_z\rho\sigma_z]$ with $(\gamma, t) \to (\gamma_S, I_n)$ for the system and $(\gamma, t) \to (\gamma_A, W_n^q)$ for the ancillas. For simplicity, we focus here on $\gamma_S = \gamma_A = \gamma$. We discuss in [58] the case where either γ_S or γ_A is zero. The goal of this toy model is to maintain the system in a state with a high amount of coherence, which we quantify using the ℓ_1 norm of coherence [62, 63] in the system, $C = |\mathrm{Tr}(\sigma_+\rho_S)|$. In this regard, both the heavy traffic and the rare arrivals regimes are deleterious. In the former, the ancillas wait too long and hence lose the coherence before they transfer it to the system. In the latter, the system is idle too often and hence loses the coherences it receives from the ancillas. To illustrate this interplay more concretely, we assume that the service times are all equal and deterministic, $S_n = \tau_{SA}$, while the interarrival times

T_n are iid and exponentially distributed, with $p_T(t) = \lambda e^{-\lambda t}$, where λ determines the rate of arrivals. The queueing properties are fully determined by $\lambda\tau_{SA}$, which is large for heavy traffic and small for rare arrivals. The quantum dynamics, on the other hand, is described by the interplay between the timescales $g\tau_{SA}$, γI_n and γW_n^q.

In Fig. 2(a) we plot the coherence after each ancilla collision for different values of $\lambda\tau_{SA}$, assuming the system starts in $\rho_S^0 = |0\rangle\langle 0|$. In the first few collisions, the coherence grows. For small $\lambda\tau_{SA}$ it remains roughly constant, while for larger $\lambda\tau_{SA}$ it drops down to zero. This happens because for large $\lambda\tau_{SA}$ the size of the queue starts to grow unboundedly. As a consequence, the waiting time for each ancilla grows and they tend to decohere more and more. A more systematic analysis is shown in Fig. 2(b), where we study the time-averaged coherence after very many collisions,

$$E(C) = \lim_{n\to\infty} \frac{1}{n} \sum_{j=1}^{n} C_j. \tag{6}$$

This is a single shot calculation; i.e., we average the coherence over a single long time run. The quantity is plotted as a function of $\lambda\tau_{SA}$, showing a clear transition at $\lambda\tau_{SA} = 1$, where $E(C)$ is nonanalytic. More interestingly, we see that C is not monotonic with $\lambda\tau_{SA}$, which reflects the non-trivial interplay of waiting and idle times. There is, therefore, an optimal value $\lambda\tau_{SA} \in (0, 1)$, which depends on the quantum dynamics parameters g and γ, for which the coherence reaches a maximum.

Another important feature of the queueing dynamics is that, in general, the system will never reach a steady state, in the sense that the long-time dynamics will cause the system state to fluctuate for arbitrarily long times. We illustrate this in Fig. 2(c), where we plot the single-shot variance of the coherence, computed in the long-time limit:

$$\mathrm{var}(C) = \lim_{n\to\infty} \frac{1}{n-1} \sum_{j=1}^{n} [C_n - E(C)]^2. \tag{7}$$

Following what happened to the average, var(C) is also nonanalytic at $\lambda\tau_{SA} = 1$. We see that for $\lambda\tau_{SA} > 1$ the fluctuations tend exactly to zero. This state coincides with the homogenization problem of Ref. [18], except that the system homogenizes to the maximally mixed state since the ancillas fully decohere. Conversely, for $\lambda\tau_{SA} < 1$ the fluctuations are non-zero, even in the long-time limit. This happens because in this regime the queue randomly alternates between idle and busy periods, as depicted in Fig. 1(e). During idle periods, the system decoheres. During busy periods, it absorbs some coherence from the ancillas.

Conclusions.–We have introduced a new dynamical model of open quantum dynamics, in which a system interacts sequentially with ancillas, in a way that is governed by a classical controller. The only assumption is that the system interacts only with one ancilla at a time. All other dynamical properties are established by the choice of interarrival and service times T_n and S_n, as well as the quantum maps $\mathcal{U}_{SA}, \mathcal{E}_A$ and $\mathcal{E}_S$. This framework therefore greatly generalizes collision models, containing previously studied QCMs as particular/limiting cases. In this Letter we aimed to illustrate the types of new dynamical rules that might emerge from this framework by studying a qubit model of coherence transfer and showing how decoherence can lead to non-trivial phases of the system's steady state.

Our results open up various avenues of research. Notably, there is still much to be explored about the map (4), including particular cases that might allow for analytical solutions, or other types of competing dynamics that could lead to interesting behaviors. In addition, the basic building blocks introduced here naturally lead to various other dynamical models. First, one could allow the ancillas to interact while in the queue. Second, one can introduce priority mechanisms, where certain ancillas are flagged as priorities, and therefore allowed to skip the queue entirely [64–66]. Third, one could study pairwise queues, where ancillas from each queue interact with one another in a pairwise fashion. This closely matches the quantum computations with neutral atom arrays [13]. Fourth, one could introduce mechanisms in which the quantum dynamics also affect the classical queue. In Eq. (4) the classical queue dynamics affects the quantum properties, but not vice-versa. One way to change that is, for example, to have the system-ancilla service time be determined by the occurrence of a quantum jump in the system (e.g. a photon is emitted).

Acknowledgments.–The authors acknowledge fruitful discussions with Gabriele De Chiara, Patrick Potts, Felix Binder, Felipe Pereira-Alves, Felipe Picoli, and Abhaya Hegde.

* gfiusa@ur.rochester.edu

[1] C. Gerry and P. Knight, *Introductory Quantum Optics* (Cambridge University Press, 2005).
[2] H. Walther, B. T. H. Varcoe, B.-G. Englert, and T. Becker, Reports on Progress in Physics **69**, 1325–1382 (2006).
[3] H. J. Carmichael, Physical Review Letters **70**, 2273–2276 (1993).
[4] C. W. Gardiner, Physical Review Letters **70**, 2269–2272 (1993).
[5] K. Stannigel, P. Rabl, and P. Zoller, New Journal of Physics **14**, 063014 (2012).
[6] J. Roßnagel, O. Abah, F. Schmidt-Kaler, K. Singer, and E. Lutz, Physical Review Letters **112** (2014), 10.1103/physrevlett.112.030602.
[7] W. Niedenzu, V. Mukherjee, A. Ghosh, A. G. Kofman, and G. Kurizki, Nature Communications **9** (2018), 10.1038/s41467-017-01991-6.
[8] N. R. Lee, Y. Guo, A. Y. Cleland, E. A. Wollack, R. G. Gruenke, T. Makihara, Z. Wang, T. Rajabzadeh, W. Jiang, F. M. Mayor, P. Arrangoiz-Arriola, C. J. Sarabalis, and A. H. Safavi-Naeini, PRX Quantum **4** (2023), 10.1103/prxquantum.4.040342.
[9] M. Pechal, P. Arrangoiz-Arriola, and A. H. Safavi-Naeini, Quantum Science and Technology **4**, 015006 (2018).
[10] C. T. Hann, C.-L. Zou, Y. Zhang, Y. Chu, R. J. Schoelkopf, S. Girvin, and L. Jiang, Physical Review Letters **123** (2019), 10.1103/physrevlett.123.250501.
[11] C. Chamberland, K. Noh, P. Arrangoiz-Arriola, E. T. Camp-

bell, C. T. Hann, J. Iverson, H. Putterman, T. C. Bohdanowicz, S. T. Flammia, A. Keller, G. Refael, J. Preskill, L. Jiang, A. H. Safavi-Naeini, O. Painter, and F. G. Brandão, PRX Quantum **3** (2022), 10.1103/prxquantum.3.010329.
[12] D. Bluvstein, H. Levine, G. Semeghini, T. T. Wang, S. Ebadi, M. Kalinowski, A. Keesling, N. Maskara, H. Pichler, M. Greiner, V. Vuletić, and M. D. Lukin, Nature **604**, 451–456 (2022).
[13] D. Bluvstein, S. J. Evered, A. A. Geim, S. H. Li, H. Zhou, T. Manovitz, S. Ebadi, M. Cain, M. Kalinowski, D. Hangleiter, J. P. Bonilla Ataides, N. Maskara, I. Cong, X. Gao, P. Sales Rodriguez, T. Karolyshyn, G. Semeghini, M. J. Gullans, M. Greiner, V. Vuletić, and M. D. Lukin, Nature **626**, 58–65 (2023).
[14] S. Ebadi, T. T. Wang, H. Levine, A. Keesling, G. Semeghini, A. Omran, D. Bluvstein, R. Samajdar, H. Pichler, W. W. Ho, S. Choi, S. Sachdev, M. Greiner, V. Vuletić, and M. D. Lukin, Nature **595**, 227–232 (2021).
[15] S. Ebadi, T. T. Wang, H. Levine, A. Keesling, G. Semeghini, A. Omran, D. Bluvstein, R. Samajdar, H. Pichler, W. W. Ho, S. Choi, S. Sachdev, M. Greiner, V. Vuletić, and M. D. Lukin, Nature **595**, 227–232 (2021).
[16] H. J. Manetsch, G. Nomura, E. Bataille, K. H. Leung, X. Lv, and M. Endres, (2024), arXiv:2403.12021v2 [quant-ph].
[17] J. Rau, Physical Review **129**, 1880–1888 (1963).
[18] M. Ziman, P. Štelmachovič, V. Bužek, M. Hillery, V. Scarani, and N. Gisin, Physical Review A **65** (2002), 10.1103/physreva.65.042105.
[19] M. Ziman and V. Bužek, Physical Review A **72** (2005), 10.1103/physreva.72.022110.
[20] L. Bruneau, A. Joye, and M. Merkli, Journal of Mathematical Physics **55** (2014), 10.1063/1.4879240.
[21] D. Grimmer, D. Layden, R. B. Mann, and E. Martín-Martínez, Physical Review A **94** (2016), 10.1103/physreva.94.032126.
[22] S. Campbell and B. Vacchini, Europhysics Letters **133**, 60001 (2021).
[23] F. Ciccarello, S. Lorenzo, V. Giovannetti, and G. M. Palma, Physics Reports **954**, 1–70 (2022).
[24] S. Lorenzo, F. Ciccarello, and G. M. Palma, Physical Review A **96** (2017), 10.1103/physreva.96.032107.
[25] G. De Chiara and M. Antezza, Physical Review Research **2** (2020), 10.1103/physrevresearch.2.033315.
[26] P. Taranto, F. Bakhshinezhad, P. Schüttelkopf, F. Clivaz, and M. Huber, Physical Review Applied **14** (2020), 10.1103/physrevapplied.14.054005.
[27] S. Campbell, F. Ciccarello, G. M. Palma, and B. Vacchini, Physical Review A **98** (2018), 10.1103/physreva.98.012142.
[28] D. A. Chisholm, G. García-Pérez, M. A. C. Rossi, G. M. Palma, and S. Maniscalco, New Journal of Physics **23**, 033031 (2021).
[29] M. Cattaneo, G. L. Giorgi, R. Zambrini, and S. Maniscalco, Open Systems & Information Dynamics **29** (2022), 10.1142/s1230161222500159.
[30] M. Cattaneo, G. De Chiara, S. Maniscalco, R. Zambrini, and G. L. Giorgi, Physical Review Letters **126** (2021), 10.1103/physrevlett.126.130403.
[31] G. Guarnieri, D. Morrone, B. Çakmak, F. Plastina, and S. Campbell, Physics Letters A **384**, 126576 (2020).
[32] G. De Chiara, G. Landi, A. Hewgill, B. Reid, A. Ferraro, A. J. Roncaglia, and M. Antezza, New Journal of Physics **20**, 113024 (2018).
[33] F. V. Melo, N. Sá, I. Roditi, A. M. Souza, I. S. Oliveira, R. S. Sarthour, and G. T. Landi, Physical Review A **106** (2022), 10.1103/physreva.106.032410.
[34] F. L. S. Rodrigues, G. De Chiara, M. Paternostro, and G. T. Landi, Physical Review Letters **123** (2019), 10.1103/physrevlett.123.140601.
[35] S. Cusumano, V. Cavina, M. Keck, A. De Pasquale, and V. Giovannetti, Physical Review A **98** (2018), 10.1103/physreva.98.032119.
[36] S. Lorenzo, F. Ciccarello, and G. M. Palma, Physical Review A **96** (2017), 10.1103/physreva.96.032107.
[37] S. Campbell, F. Ciccarello, G. M. Palma, and B. Vacchini, Physical Review A **98** (2018), 10.1103/physreva.98.012142.
[38] R. McCloskey and M. Paternostro, Physical Review A **89** (2014), 10.1103/physreva.89.052120.
[39] S. Kretschmer, K. Luoma, and W. T. Strunz, Physical Review A **94** (2016), 10.1103/physreva.94.012106.
[40] N. K. Bernardes, A. R. R. Carvalho, C. H. Monken, and M. F. Santos, Physical Review A **90** (2014), 10.1103/physreva.90.032111.
[41] A. Shu, S. Seah, and V. Scarani, Physical Review A **102** (2020), 10.1103/physreva.102.042417.
[42] S. Seah, S. Nimmrichter, D. Grimmer, J. P. Santos, V. Scarani, and G. T. Landi, Physical Review Letters **123** (2019), 10.1103/physrevlett.123.180602.
[43] J. Tabanera, I. Luque, S. L. Jacob, M. Esposito, F. Barra, and J. M. R. Parrondo, New Journal of Physics **24**, 023018 (2022).
[44] P. Strasberg, Physical Review E **100** (2019), 10.1103/physreve.100.022127.
[45] F. Barra, Scientific Reports **5** (2015), 10.1038/srep14873.
[46] J. A. Gross, C. M. Caves, G. J. Milburn, and J. Combes, Quantum Science and Technology **3**, 024005 (2018).
[47] M. Rossi, L. Mancino, G. T. Landi, M. Paternostro, A. Schliesser, and A. Belenchia, Physical Review Letters **125** (2020), 10.1103/physrevlett.125.080601.
[48] G. T. Landi, M. Paternostro, and A. Belenchia, PRX Quantum **3** (2022), 10.1103/prxquantum.3.010303.
[49] S. Osnaghi, P. Bertet, A. Auffeves, P. Maioli, M. Brune, J. M. Raimond, and S. Haroche, Physical Review Letters **87** (2001), 10.1103/physrevlett.87.037902.
[50] Z. Gong, R. Hamazaki, and M. Ueda, Physical Review Letters **120** (2018), 10.1103/physrevlett.120.040404.
[51] M. Maffei, P. A. Camati, and A. Auffèves, Entropy **24**, 151 (2022).
[52] F. Ciccarello, Quantum Measurements and Quantum Metrology **4** (2017), 10.1515/qmetro-2017-0007.
[53] L. Kleinrock, *Queueing Systems, Volume I*, A Wiley-Interscience publication No. v. 1 (Wiley, 1974).
[54] D. Gross, J. Shortle, J. Thompson, and C. Harris, *Fundamentals of Queueing Theory*, Wiley Series in Probability and Statistics (Wiley, 2011).
[55] J. Cohen, *The Single Server Queue*, North-Holland series in applied mathematics and mechanics (North-Holland Publishing Company, 1969).
[56] The framework we develop does not rely on their statistical properties. In the simplest case (known as a G/G/1 queue) the $\{T_n, S_n\}$ are taken to be independent and identically distributed (iid) random variables, drawn from two distributions $p_T(t)$ and $p_S(s)$.
[57] D. V. Lindley, Proceedings of the Cambridge Philosophical Society **48**, 277 (1952).
[58] See Supplemental Material for more details.
[59] The number of ancillas that have arrived up to time t is $N_{\rm arr}(t) = \sum_{n=1}^{\infty} \theta(t - t_n)$, where θ is the Heaviside function. The number of ancillas that have left the system up to time t is $N_{\rm left}(t) = \sum_{n=1}^{\infty} \theta(t - s_n)$. Hence, the population of ancillas in the queue, including the one that might be interacting with the system, can be calculated as $\max\{0, N_{\rm arr}(t) - N_{\rm left}(t)\}$.

[60] P. Strasberg, G. Schaller, T. Brandes, and M. Esposito, Physical Review X **7** (2017), 10.1103/physrevx.7.021003.

[61] F. Ciccarello, G. M. Palma, and V. Giovannetti, Physical Review A **87** (2013), 10.1103/physreva.87.040103.

[62] T. Baumgratz, M. Cramer, and M. Plenio, Physical Review Letters **113** (2014), 10.1103/physrevlett.113.140401.

[63] A. Streltsov, G. Adesso, and M. B. Plenio, Reviews of Modern Physics **89** (2017), 10.1103/revmodphys.89.041003.

[64] A.-L. Barabási, Nature **435**, 207–211 (2005).

[65] A. Vázquez, Physical Review Letters **95** (2005), 10.1103/physrevlett.95.248701.

[66] A. Vázquez, J. G. Oliveira, Z. Dezsö, K.-I. Goh, I. Kondor, and A.-L. Barabási, Physical Review E **73** (2006), 10.1103/physreve.73.036127.

Supplemental Material

COMMENTS ABOUT QUEUES AND DERIVATION OF LINDLEY'S EQUATION

A queueing process is defined by the interarrival times T_n and the service times S_n. Although the recursion relations (1) and (2) effectively provide a way to "solve" the queue by calculating the idle times I_n and waiting times W_n^q for every customer (ancilla), they make no mention toward the distributions of those quantities. Therefore, a natural question to address is what the distributions of I_n and W_n^q look like. One aspect that makes this analysis nontrivial and interesting is the fact that both distributions are a sum of a discrete part and a continuous smooth part, e.g.,

$$\begin{aligned} P(W_n^q) &= P_0\delta(W_n^q) + f(W_n^q), \\ P(I_n) &= I_0\delta(I_n) + g(I_n), \end{aligned}$$

where P_0 and I_0 account for the nonvanishing probability that the ancilla has no waiting time (i.e. finds the queue empty upon arrival) or the system has no idle time, respectively. Functions f (g) denote some smooth function that depends on W_n^q (I_n). In what follows, we analyze some of the richness behind the distributions $P(W_n^q)$ and $P(I_n)$ in the case where both T_n and S_n are independent and identically distributed (iid) random variables.

Let us denote the cumulative distribution function (CDF) of the waiting times as

$$F_n(x) = P(W_n^q \leqslant x). \tag{S1}$$

Here it is convenient to introduce $U_n = S_n - T_n$, which is an iid random variable distributed according to a probability density function $p(u)$. It follows,

$$\begin{aligned} F_{n+1}(x) &= P(W_{n+1}^q \leqslant x) \\ &= P(W_{n+1}^q = 0) + P(0 < W_{n+1}^q \leqslant x) \\ &= P(W_n^q + U_n \leqslant 0) + P(0 < W_n^q + U_n \leqslant x) \\ &= P(W_n^q + U_n \leqslant x) \\ &= \int_{-\infty}^{x} P(W_n^q \leqslant x - u)p(u)du, \end{aligned}$$

where we conclude, after changing variables to $v = x - u$,

$$F_{n+1}(x) = \int_0^\infty F_n(v)p(x-v)dv. \tag{S2}$$

This result is known as the Lindley equation. It allows us to specify the CDF of any customer in terms of only the CDF of the previous customer. Given that $F_n(x)$ are CDFs, they have the following properties: (i) $F_1(x) = 1,\ \forall\ x \geqslant 0$, which follows from $W_1^q \equiv 0$; (ii) $F_n(x \to \infty) = 1$; (iii) $F_n(0)$ is generally not zero, since this represents the probability that the customer finds the queue empty and does not have to wait.

Following the same procedure, we use the recursion relations (1) and (2) to derive a result where the idle time statistics can be calculated from the waiting time probabilities $F_n(x)$. The starting point is

$$P(I_{n+1} \leqslant x) = P(I_{n+1} = 0) + P(0 < I_{n+1} \leqslant x),$$

applying the recursion relations (1) and (2),

$$\begin{aligned} P(I_{n+1} \leqslant x) &= P(W_n^q + U_n = 0) + P(0 < -(W_n^q + U_n \leqslant x) \\ &= P(W_n^q + U_n \geqslant 0) + P(-x \leqslant W_n^q + U_n < 0) \\ &= P(-x \leqslant W_n^q + U_n) \\ &= P(W_n^q \geqslant -x - U_n) \quad (x \geqslant 0), \end{aligned}$$

now we use the fact that U_n is an iid random variable with a PDF given by $p(u)$. It follows

$$\begin{aligned} P(I_{n+1} \leqslant x) &= \int_{\infty}^{-\infty} du\ p(u) P(W_n^q \geqslant -x-u) \\ &= \int_{-\infty}^{\infty} du\ p(u)\left[1 - P(W_n^q \leqslant -x-u)\right] \\ &= 1 - \int_{-\infty}^{-x} du\ p(u) F_n(-x-u), \end{aligned}$$

so the result becomes

$$G_{n+1}(x) = P(I_{n+1} \leqslant x) = 1 - \int_0^{\infty} dv\ p(-x-v) F_n(v), \tag{S3}$$

with $v = -x - u$. To the best of the authors' knowledge, this result of queueing theory has never been reported in the literature before.

STEADY STATE SOLUTION FOR THE DETERMINISTIC QCM

We further elaborate on the steady state solution of the deterministic QCM in Fig. 1(b) from the queued QCM. Here, we work in the "heavy traffic" limit, where $S_n \gg T_n$. This means that ancillas arrive much more quickly than the system can serve them. As a consequence, the queue quickly builds up, and the system will never be idle ($I_n = 0$), so $\mathcal{E}_S$ is the identity. To make a connection with typical deterministic QCM dynamics, we also assume that there is no waiting time dynamics for the ancillas. The dynamics from Eq. (4) then reduce to

$$\rho_S^n = \mathrm{Tr}_A\left[\mathcal{U}_{SA}(S_n)(\rho_S^{n-1} \otimes \rho_A)\right]. \tag{S4}$$

The expectation value of the state after the collision with the n-th ancilla is then given by

$$\begin{aligned} E[\rho_S^n] &= \int dS_1 ... dS_n P(S_1)...P(S_n)\ \mathrm{Tr}_A[\mathcal{U}_{SA}(S_n)(\rho_S^{n-1} \otimes \rho_A)] \\ &= \int dS_n P(S_n)\ \mathrm{Tr}_A[\mathcal{U}_{SA}(S_n)(E[\rho_S^{n-1}] \otimes \rho_A)], \end{aligned}$$

and the steady state follows

$$E[\rho_S^{ss}] = \int ds P(s)\ \mathrm{Tr}_A[\mathcal{U}_{SA}(s)(E[\rho_S^{ss}] \otimes \rho_A)] \tag{S5}$$

$$= \Phi[E(\rho_S^{ss})]. \tag{S6}$$

Note that the steady state solution is reached irrespective of the properties of the service times S_n. However, to recover the standard formulation, we may assume that $S_n = \tau_{SA}$, and that the system-ancilla map is unitary, of the form $\mathcal{U}_{SA}(\tau_{SA})[\bullet] = e^{-iH_{SA}\tau_{SA}} \bullet e^{iH_{SA}\tau_{SA}}$, where H_{SA} is the system-ancilla Hamiltonian. We emphasize, however, that the steady state solution in the heavy traffic regime does not rely on this last assumption. In the case that $S_n = \tau_{SA}$, the integration (S5) becomes trivial.

RECOVERING THE STOCHASTIC QCM FROM THE QUEUED QCM

Here, we show how one recovers the stochastic model in Fig. 1(a) from the queued QCM (4). Here, we work in the regime of "rare arrivals", where $T_n \gg S_n$. This imples, following Eq. (2), that $W_{n+1}^q \simeq 0$ and $I_{n+1} \simeq T_n$. The queue is empty most of the time, so ancillas arriving do not have to wait. The system is evolving, most of the time, under the idle map $\mathcal{E}_S(T_{n-1})$, which now depends only on the interarrival times T_{n-1}. We also assume that $\mathcal{U}_{SA}(S_n) = \mathcal{U}_{SA}$ is still non-trivial, even for very small S_n. Under these assumptions, Eq. (4) reduces to

$$\rho_S^n = \mathrm{Tr}_A\left\{\mathcal{U}_{SA}\left[\mathcal{E}_S(T_{n-1})[\rho_S^{n-1}] \otimes \rho_A\right]\right\}, \tag{S7}$$

while Eq. (3) reduces to $s_n = \sum_{j=1}^n T_j$.

It is clear that in this limit any stochasticity in the model will reside in the statistics of T_{n-1}. The usual stochastic QCMs correspond to the case where the interarrival times T_n are iid with distribution $p_T(t)$. A more common representation of stochastic QCMs is obtained if one switches to a time ensemble, where we describe the state of the system at a definite time, but allow the number of collisions to vary. This can be accomplished by defining

$$\varrho_S^{(n)}(t) := E[\rho_S^n \delta(t - s_{n-1})]/E[\delta(t - s_{n-1})], \tag{S8}$$

where the ensemble average is over the joint realization of all interarrival times. The state $\varrho_S^{(n)}(t)$ now describes the evolution of the system over some time t, where the number of collisions n can vary. Explicitly, the expectation values are given by

$$\begin{aligned} E[\cdot] &= \int dT_1 ... dT_{n-1} (\cdot) P(T_1) ... P(T_{n-1}) \\ &\equiv \int dT_{1...n-1} (\cdot) P(T_{1...n-1}), \end{aligned}$$

it then follows

$$\varrho_S^{(n)}(t) = \frac{1}{E[\delta(t - s_{n-1})]} \int dT_{1...n-1} P(T_{1...n-1}) \delta(t - s_{n-1}) \mathrm{Tr}_A \left[\mathcal{U}_{SA} \left(\mathcal{E}_S(T_{n-1})(\rho_S^{n-1}) \otimes \rho_A \right) \right],$$

where the only term that depends on the interarrival time T_{n-1} is the idle dynamics channel. On top of that, we can substitute $s_{n-1} = s_{n-2} + I_{n-1} + S_{n-1} = s_{n-2} + T_{n-2}$ in the delta inside the integral, so we get

$$\begin{aligned} \varrho_S^{(n)}(t) &= \frac{1}{E[\delta(t - s_{n-1})]} \int dT_{n-1} P(T_{n-1}) \mathrm{Tr}_A [\mathcal{U}_{SA} (\mathcal{E}_S(T_{n-1}) \left(\int P(T_{1...n-2}) \rho_S^{n-1} \delta(t - s_{n-2} - T_{n-2}) dT_{1...n-2} \right) \otimes \rho_A)], \\ &= \frac{E[\delta(t - s_{n-2})]}{E[\delta(t - s_{n-1})]} \int dT_{n-1} P(T_{n-1}) \mathrm{Tr}_A \left[\mathcal{U}_{SA} \left(\mathcal{E}_S(T_{n-1}) [\varrho_S^{(n-1)}(t - T_{n-1})] \otimes \rho_A \right) \right]. \end{aligned}$$

By defining $\tilde{\varrho}_S^{(n)}(t) := \varrho_S^{(n)}(t) E[\delta(t - s_{n-1})]$ and changing variables $T_{n-1} \equiv t'$, we obtain the final result

$$\tilde{\varrho}_S^{(n)}(t) = \int dt' p_T(t') \mathrm{Tr}_A \left[\mathcal{U}_{SA} \left(\mathcal{E}_S(t') [\tilde{\varrho}_S^{(n-1)}(t - t')] \otimes \rho_A \right) \right], \tag{S9}$$

where $P(t') \equiv p_T(t')$. Eq. (S9) describes precisely the familiar representation used in studies of stochastic QCMs [60].

FURTHER EXAMPLES OF THE TOY MODEL DYNAMICS

In the main text, we considered a qubit toy model of coherence transfer where both the system and the ancillas underwent a dephasing channel during their idle and waiting dynamics, respectively. The goal was to prepare ancillas with coherence and observe the coherence transfer to the system through the partial SWAP interactions as a function of $\lambda\tau_{SA}$. Here, we discuss two particular cases of this model. In the first, we consider that there is dephasing only in the system, so the idle channel is $\mathcal{E}_S(t)[\rho] = \frac{1}{2}[(1 + e^{-\gamma t})\rho + (1 - e^{-\gamma t})\sigma_z \rho \sigma_z]$ with $(\gamma, t) \to (\gamma_S, I_n)$, and the waiting time channel is the identity ($\gamma_A = 0$). In the second, we have a dephasing channel only for the ancillas, so the idle channel is the identity ($\gamma_S = 0$) and the waiting time channel is $\mathcal{E}_A(t)[\rho] = \frac{1}{2}[(1 + e^{-\gamma t})\rho + (1 - e^{-\gamma t})\sigma_z \rho \sigma_z]$ with $(\gamma, t) \to (\gamma_A, W_n^q)$.

Let us begin by discussing the first extension, where the dephasing channel describes only the idle system dyamics. In Fig. S1(a) we plot the coherence after each ancilla collision for different values of $\lambda\tau_{SA}$, assuming the system starts in $\rho_S^0 = |0\rangle\langle 0|$ and that ancillas are iid and prepared in the state $\rho_A = |+\rangle\langle +|$. In this setup, ancillas always have coherence $1/2$ whereas the system loses coherence whenever it becomes idle. This competition gives rise to the oscillations observed in Fig. S1(a) for $\lambda\tau_{SA} < 1$. Since there is no other mechanism in which the system may obtain coherence, we observe that the average coherence is monotonically increasing with respect to $\lambda\tau_{SA}$, see Fig. S1(b). This result is intuitive in the sense that if the arrivals are more frequent, the system is less and less idle, hence it loses less and less coherence. Once $\lambda\tau_{SA} > 1$ is reached, the system becomes permanently busy and the model recovers the homogenization problem, where

$$\lim_{n \to \infty} \rho_S^n = \rho_A,$$

and a true steady state is reached because the fluctuations go to zero, see Fig. S1(c). This model captures the small $\lambda\tau_{SA}$ behavior ("left" part of Fig. 2(b)) of the general qubit model presented for the QQCM, where we observe that C is monotonically increasing with $\lambda\tau_{SA}$ before the inflection point is reached.

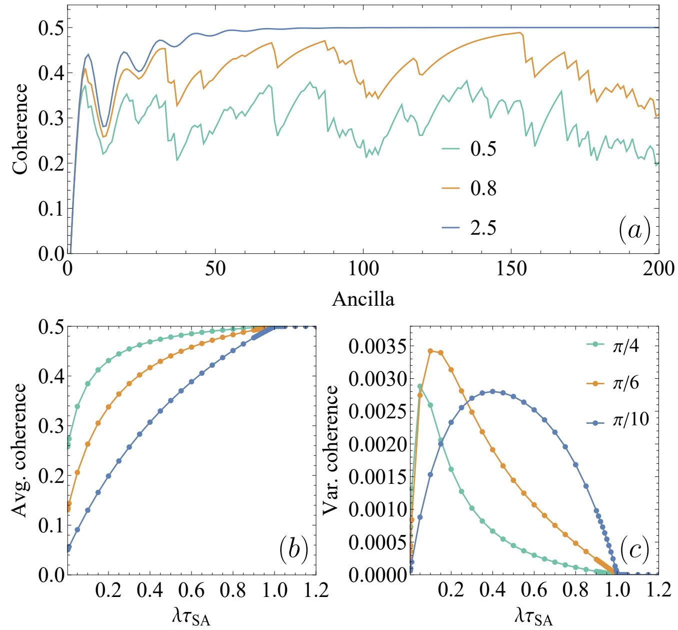

FIG. S1. System ℓ_1 norm of coherence C in the modified qubit toy model, where there is only idle dynamics describing a dephasing channel ($\gamma_A = 0$). (a) C_n as a function of ancilla number (evaluated at the times each ancilla leaves the process), for different values of $\lambda\tau_{SA}$, with $\gamma_S\tau_{SA} = 0.05$ and $g\tau_{SA} = \pi/12$. (b) Single-shot time average and (c) variance of the coherence in the long-time limit as a function of $\lambda\tau_{SA}$, for different values of $g\tau_{SA}$, with $\gamma_S\tau_{SA} = 0.05$.

In the second extension, we consider that the dephasing channel describes only the ancilla waiting time dynamics. In Fig. S2(a) we plot the coherence after each ancilla collision for different values of $\lambda\tau_{SA}$, assuming the system starts in $\rho_S^0 = |0\rangle\langle 0|$ and that ancillas are iid and prepared in the state $\rho_A = |+\rangle\langle +|$. In this setup, ancillas lose coherence depending on how long they wait in the queue, but the system does not lose any coherence while it is idle. The coherence transfer, therefore, becomes a competition between the partially dephased ancillas and the remaining coherence of the system, which is acquired through previous partial SWAP interactions. This new kind of competition effect gives rise to a peculiar feature that is observed in Fig. S2(b): the average coherence is independent of the partial SWAP coupling. This is an artifact of the very long time behavior. Since the system does not lose any coherence when it is idle, what effectively dictates how much coherence it will have in long times is how strongly dephased the ancillas are. For smaller values of $\lambda\tau_{SA}$, even if ancillas arrive very rarely, they lose very little coherence, so the partial SWAPs will eventually lead the system to a high coherence state. As the frequency of arrivals increases, the queue starts to pile up and as a consequence, the long time behavior coherence of the system will be smaller because whenever it interacts it will be with more and more dephased ancillas that are waiting longer in the queue. Once $\lambda\tau_{SA} > 1$ is reached, the queue grows indefinitely and every ancilla is completely dephased. As a consequence, the system loses all coherence. The model now homogenizes to the completely dephased ancilla state, which is the identity:

$$\lim_{n\to\infty} \rho_S^n = \mathcal{E}_A(t \to \infty)[\rho_A] = \frac{1}{2}\mathbb{I}.$$

Note that this is a steady state of the dynamics because the fluctuations vanish, see Fig. S2(c). This model captures the large $\lambda\tau_{SA}$ behavior (including values below and above the $\lambda\tau_{SA} = 1$ transition, i.e. the "right" part of Fig. 2(b)) of the general qubit model we presented for the QQCM, where we observe that C is monotonically decreasing with $\lambda\tau_{SA}$ before reaching $\lambda\tau_{SA} = 1$, and zero after.

Those two examples where we turn on only one kind of dynamics at a time illustrate one feature of the full QQCM example we discussed in the main text, namely, that there is value $\lambda\tau_{SA} \in (0, 1)$ that maximizes the average coherence. This effect is a direct competition between the two channels acting simultaneously. As we observed in the two examples discussed here, turning off the waiting time dynamics essentially describes the small $\lambda\tau_{SA}$ regime while turning off the idle dynamics effectively describes the large $\lambda\tau_{SA}$ regime. In the former, we see that the coherence transfer is monotonically increasing with $\lambda\tau_{SA}$ whereas in the latter it is monotonically decreasing. The optimal coherence point arises as an inflection point between those two behaviors, which are directly related to the queue. In both examples, the transition is still present at $\lambda\tau_{SA} = 1$, where the average and the variance of the coherence are nonanalytic at this point.

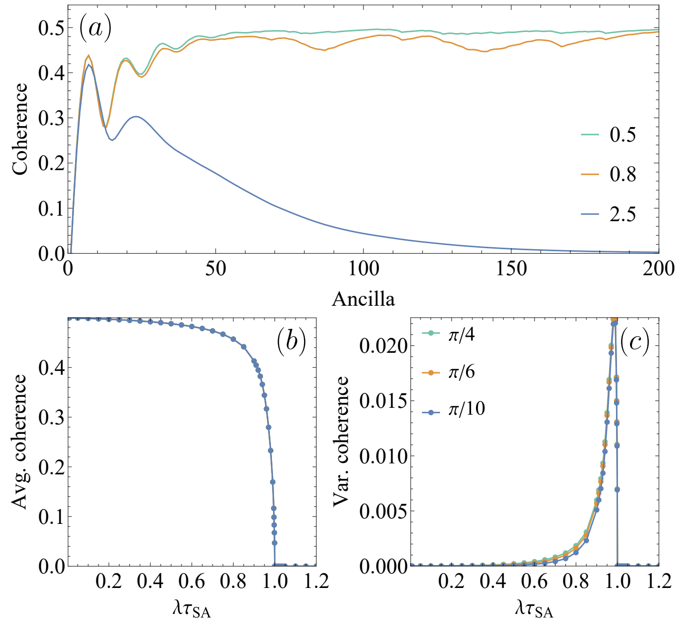

FIG. S2. System ℓ_1 norm of coherence C in the modified qubit toy model, where there is only waiting time dynamics describing a dephasing channel. (a) C_n as a function of ancilla number (evaluated at the times each ancilla leaves the process), for different values of $\lambda\tau_{SA}$, with $\gamma\tau_{SA} = 0.05$ and $g\tau_{SA} = \pi/12$. (b) Single-shot time average and (c) variance of the coherence in the long-time limit as a function of $\lambda\tau_{SA}$, for different values of $g\tau_{SA}$, with $\gamma\tau_{SA} = 0.05$.